

# 简谐荷载作用下非饱和土地基中波阻板 隔振效果研究

张 猛<sup>1</sup>, 马 强<sup>1,2</sup>

(1. 青海大学土木工程学院, 青海 西宁 810016; 2. 青海省建筑节能材料与工程安全重点实验室, 青海 西宁 810016)

**摘要:** 鉴于非饱和土地基振动问题的普遍性和复杂性, 环境振动下非饱和土地基振动控制已成为土动力学的研究热点。基于单相弹性介质和非饱和多孔介质理论, 对简谐荷载作用下非饱和土地基中设置单相固体波阻板的隔振效果进行了研究。考虑地表排水排气的边界条件, 利用 Fourier 积分变换和 Helmholtz 矢量分解原理, 建立了动荷载作用下地基动力响应的计算列式。分析了非饱和土地基中土体饱和度、荷载频率、波阻板的埋深、厚度以及弹性模量对其隔振性能的影响规律。结果表明: 非饱和土地基中设置波阻板能够取得很好的隔振效果。地表位移幅值随饱和度和波阻板埋深的减小而显著降低, 随荷载频率、波阻板的厚度和弹性模量的增大而明显减小。

**关键词:** 非饱和土地基; 波阻板; 隔振效果; 动力响应

**中图分类号:** TU435 **文献标志码:** A **文章编号:** 1004-4523(2023)04-1136-10

**DOI:** 10.16385/j.cnki.issn.1004-4523.2023.04.027

## 引 言

随着城镇化建设和现代化工业的迅速发展, 各种人工振动引起的振动污染愈加频繁, 如轨道交通、爆破等工程活动工作时产生的振动对各种精密仪器的正常运作以及人们的生活环境和工作环境产生了诸多不利影响。因此, 对人工振动引起的振动传播过程和地基的振动规律进行分析研究, 从而找到有效的减振隔振措施具有重要的实际意义, 隔振理论和方法成为土动力学研究的热点。

在既有振源与保护区之间设立屏障来切断弹性波的传播路径, 消耗振动能量, 降低振动幅度, 是目前国际上普遍采用的隔振措施。Woods<sup>[1]</sup>最早通过现场原位试验对远场被动隔振和近场主动隔振进行了研究, 提出了屏障隔振设计的基本准则, 给出了衡量屏障隔振效果的系数——振幅衰减系数。之后国内外的学者对各种隔振屏障的减隔振性能开展了大量的研究工作<sup>[2-12]</sup>。根据隔振屏障的形式, 高广运<sup>[12]</sup>按几何特性进一步将屏障分为连续屏障(如空沟、填充沟等)和非连续屏障(如桩列和板桩等)。

除了以上所述的屏障隔振外, 另一种可供选择的隔振屏障是在振源或被保护结构下一定深度内埋置波阻板进行隔振。Chouw 等<sup>[13]</sup>最先分析了弹性地基中波阻板主动和被动隔振效果, 并对填充沟和

波阻板的被动隔振效果进行了对比分析, 结果表明波阻板的隔振效果要优于填充沟。Takemiya 等<sup>[14]</sup>采用波阻板研究了基岩上单一土层中群桩基础激励时的隔振效果, 结果表明波阻板是一种有效的隔振措施。周凤玺等<sup>[15]</sup>研究了弹性地基中含液饱和多孔波阻板的隔振性能。马强等<sup>[16]</sup>建立了弹性地基中功能梯度波阻板的地基隔振体系, 研究表明梯度波阻板能有效地降低振动的振幅。田抒平等<sup>[17]</sup>和高盟等<sup>[18]</sup>提出一种带孔波阻板填充 Duxseal 的联合隔振方法(简称 DXWIB), 通过试验研究发现较浅埋深的 DXWIB 屏障可以有效地减小地表竖向位移。高广运等<sup>[19-20]</sup>针对饱和土地基模型, 对轨道交通荷载作用下饱和土地基中波阻板的隔振性能进行了研究。随后基于改进的三维边界有限元模型, Gao 等<sup>[21]</sup>研究了饱和土体中波阻板的隔振效果, 分析了土地基-波阻板相互作用的问题。徐长节等<sup>[22]</sup>建立了饱和土地基中夹水混凝土复合屏障的计算模型, 结果表明, 入射波的入射角度及屏障的弹性模量对屏障的隔振效果影响最为明显。

综上所述, 目前关于波阻板隔振屏障的研究大都限于单相弹性地基与饱和土地基中。然而, 非饱和土地基才是自然界中土体更为普遍的存在状态。地基振动由于振源位置、振源类型以及地基物理学性质的不同而产生不同的波场特性, 其振动的传播过程和衰减规律也不相同。因此, 研究非饱和土

地基中波阻板的减振隔振效果具有更普遍意义。本文基于非饱和多孔介质的控制方程,建立了非饱和土地基中设置均质波阻板的数学模型,利用Fourier积分变换,通过Helmholtz矢量分解原理,推导获得了土体在Fourier变换域中动力问题的位移、应力的通解。通过数值算例,研究了非饱和土地基中设置波阻板后的隔振效果,且与饱和土地基比较了隔振效果的区别,分析了非饱和土地基中饱和度、荷载频率、波阻板埋深、厚度以及波阻板弹性模量对地基隔振性能的影响规律。

## 1 控制方程

### 1.1 单向固体介质

各向同性的线弹性单相连续固体介质的控制方程:

$$(\lambda_e + \mu_e) \nabla(\nabla \cdot \mathbf{u}^e) + \mu_e \nabla^2 \mathbf{u}^e = \rho_e \ddot{\mathbf{u}}^e \quad (1)$$

式中  $\lambda_e$  和  $\mu_e$  表示固体材料的Lame弹性常数;  $\rho_e$  为固体材料密度;  $\mathbf{u}^e$  表示位移矢量。

相应的应力-位移关系为:

$$\boldsymbol{\sigma}^e = \lambda_e (\nabla \cdot \mathbf{u}^e) \mathbf{I} + \mu_e (\nabla \mathbf{u}^e + \mathbf{u}^e \nabla) \mathbf{I} \quad (2)$$

式中  $\boldsymbol{\sigma}^e$  表示单相弹性固体中的应力张量;  $\mathbf{I}$  为单位矩阵。

根据Helmholtz矢量分解原理,位移矢量  $\mathbf{u}^e$  可以用势函数表示为:

$$\mathbf{u}^e = \nabla \varphi_e + \nabla \times \psi_e \quad (3)$$

式中  $\varphi_e$  和  $\psi_e$  分别为单相固体的标量位势函数和矢量位势函数。

将式(3)代入式(1)中,整理得到弹性固体波动方程:

$$\nabla^2 \varphi_e = \frac{1}{v_p^2} \frac{\partial^2 \varphi_e}{\partial t^2}, \quad \nabla^2 \psi_e = \frac{1}{v_s^2} \frac{\partial^2 \psi_e}{\partial t^2} \quad (4)$$

式中  $v_p = \sqrt{(\lambda_e + 2\mu_e)/\rho_e}$ ,  $v_s = \sqrt{\mu_e/\rho_e}$  分别为纵波和横波的传播速度。

### 1.2 非饱和和多孔介质

考虑土体受到简谐荷载作用,在稳态情况下,所有变量都可写成:

$$f = f^* e^{i\omega t} \quad (5)$$

为了方便,后面的推导过程略去星号。基于连续介质力学和Bishop有效应力公式,徐明江等<sup>[23]</sup>提出的非饱和土的动力控制方程为:

$$\begin{aligned} \mu_p \nabla^2 \mathbf{u}^s + (\lambda_p + \mu_p) \nabla \nabla \cdot \mathbf{u}^s - \alpha \gamma \nabla p^l - \\ \alpha(1-\gamma) \nabla p^g = -\omega^2 \bar{\rho}_s \mathbf{u}^s - \omega^2 \bar{\rho}_l \mathbf{u}^l - \omega^2 \bar{\rho}_g \mathbf{u}^g \end{aligned} \quad (6a)$$

$$-\nabla p^l = b^l i \omega (\mathbf{u}^l - \mathbf{u}^s) - \omega^2 \rho_l \mathbf{u}^l \quad (6b)$$

$$-\nabla p^g = b^g i \omega (\mathbf{u}^g - \mathbf{u}^s) - \omega^2 \rho_g \mathbf{u}^g \quad (6c)$$

$$-p^l = a_{11} \nabla \cdot \mathbf{u}^s + a_{12} \nabla \cdot \mathbf{u}^l + a_{13} \nabla \cdot \mathbf{u}^g \quad (6d)$$

$$-p^g = a_{21} \nabla \cdot \mathbf{u}^s + a_{22} \nabla \cdot \mathbf{u}^l + a_{23} \nabla \cdot \mathbf{u}^g \quad (6e)$$

式中  $a_{11} \sim a_{23}$ ,  $A_{11} \sim A_{24}$ ,  $b^l$ ,  $b^g$ ,  $\alpha$ ,  $\gamma$  等系数详见文献[23];  $\mathbf{u}^s$ ,  $\mathbf{u}^l$ ,  $\mathbf{u}^g$ ,  $\bar{\rho}_s = (1-n)\rho_s$ ,  $\bar{\rho}_l = nS_r \rho_g$ ,  $\bar{\rho}_g = n(1-S_r)\rho_g$  分别为非饱和土固、液、气相的位移和相对密度;  $\rho_s$ ,  $\rho_l$ ,  $\rho_g$  分别为固、液、气相的密度;  $\omega$  为角频率;  $n$  为孔隙率;  $S_r$  为饱和度;  $\lambda_p$ ,  $\mu_p$  为非饱和土的Lame系数;  $p^l$ ,  $p^g$  分别为孔隙水压力、孔隙气压力。

非饱和土的应力-应变关系为:

$$\sigma_{ij} = \lambda_p e \delta_{ij} + 2\mu_p \varepsilon_{ij} - \delta_{ij} \alpha p \quad (7)$$

式中  $\sigma_{ij}$  为非饱和土体介质的总应力分量 ( $i, j = 1, 3$ ),  $e = \nabla \cdot \mathbf{u}^s$  为土骨架体应变,  $\delta_{ij}$  为克罗内克符号,  $\varepsilon_{ij}$  为土骨架的应变,  $p = \gamma p^l + (1-\gamma) p^g$  为等效孔隙流体压力。

将式(6d), (6e)代入式(6a), (6b)和(6c)整理后

$$\begin{aligned} \mu_p \nabla^2 \mathbf{u}^s + B_1 \nabla(\nabla \cdot \mathbf{u}^s) + B_2 \nabla(\nabla \cdot \mathbf{u}^l) + \\ B_3 \nabla(\nabla \cdot \mathbf{u}^g) = -\omega^2 \bar{\rho}_s \mathbf{u}^s - \omega^2 \bar{\rho}_l \mathbf{u}^l - \omega^2 \bar{\rho}_g \mathbf{u}^g \end{aligned} \quad (8a)$$

$$\begin{aligned} a_{11} \nabla(\nabla \cdot \mathbf{u}^s) + a_{12} \nabla(\nabla \cdot \mathbf{u}^l) + a_{13} \nabla(\nabla \cdot \mathbf{u}^g) = \\ C_1 \mathbf{u}^s + C_2 \mathbf{u}^l \end{aligned} \quad (8b)$$

$$\begin{aligned} a_{21} \nabla(\nabla \cdot \mathbf{u}^s) + a_{22} \nabla(\nabla \cdot \mathbf{u}^l) + a_{23} \nabla(\nabla \cdot \mathbf{u}^g) = \\ C_3 \mathbf{u}^s + C_4 \mathbf{u}^g \end{aligned} \quad (8c)$$

式中  $B_1 = \lambda_p + \mu_p + \alpha \gamma a_{11} + \alpha(1-\gamma) a_{21}$ ,  $B_2 = \alpha \gamma a_{12} + \alpha(1-\gamma) a_{22}$ ,  $B_3 = \alpha \gamma a_{13} + \alpha(1-\gamma) a_{23}$ ,  $C_1 = -b^l i \omega$ ,  $C_2 = b^l i \omega - \omega^2 \rho_l$ ,  $C_3 = -b^g i \omega$ ,  $C_4 = b^g i \omega - \omega^2 \rho_g$ 。

根据Helmholtz矢量分解原理,位移矢量  $\mathbf{u}^s$ ,  $\mathbf{u}^l$ ,  $\mathbf{u}^g$  可以用势函数表示为:

$$\mathbf{u}^z = \nabla \varphi_z + \nabla \times \psi_z \quad (9)$$

式中  $z = s, l, g$ ;  $\varphi_s, \varphi_l, \varphi_g$  分别为固、液、气相的标量位势函数;  $\psi_s, \psi_l, \psi_g$  分别为固、液、气相的矢量位势函数。

将式(9)代入式(8)中进行散度和旋度运算,整理可得:

$$\begin{aligned} (\mu_p + B_1) \nabla^2 \varphi_s + B_2 \nabla^2 \varphi_l + B_3 \nabla^2 \varphi_g = \\ -\omega^2 \bar{\rho}_s \varphi_s - \omega^2 \bar{\rho}_l \varphi_l - \omega^2 \bar{\rho}_g \varphi_g \end{aligned} \quad (10a)$$

$$a_{11} \nabla^2 \varphi_s + a_{12} \nabla^2 \varphi_l + a_{13} \nabla^2 \varphi_g = C_1 \varphi_s + C_2 \varphi_l \quad (10b)$$

$$a_{21} \nabla^2 \varphi_s + a_{22} \nabla^2 \varphi_l + a_{23} \nabla^2 \varphi_g = C_3 \varphi_s + C_4 \varphi_g \quad (10c)$$

$$\mu_p \nabla^2 \psi_s = -\omega^2 \bar{\rho}_s \psi_s - \omega^2 \bar{\rho}_l \psi_l - \omega^2 \bar{\rho}_g \psi_g \quad (10d)$$

$$C_1 \psi_s + C_2 \psi_l = 0 \quad (10e)$$

$$C_3\psi_s + C_4\psi_g = 0 \quad (10f)$$

## 2 位移势函数的解

考虑非饱和土地基的表面受到频率为 $\omega$ ,幅值为 $q_0$ 的竖向条形简谐荷载 $q = q_0 e^{i\omega t}$ 作用,如图1所示。在距离非饱和土地基表面深度为 $H$ 处设置厚度为 $h_w$ 的波阻板。波阻板将非饱和土地基分成I和II两部分,图1中给出了波的传播以及波幅的示意图。

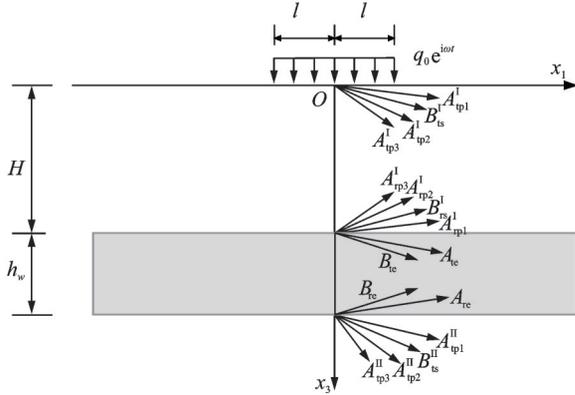


图1 简谐荷载作用下非饱和土地基设置波阻板的波传播示意图

Fig. 1 Wave propagation diagram of wave impeding block in unsaturated soil under harmonic load

### 2.1 单向固体介质的解

对空间变量 $x_1$ 进行Fourier变换:

$$\tilde{f}(\xi, x_3) = \int_{-\infty}^{\infty} f(x_1, x_3) e^{-i\xi x_1} dx_1 \quad (11)$$

将式(5)和式(11)代入方程(4)中,经过Fourier变换整理可得:

$$\frac{d^2 \tilde{\varphi}_e}{dx_3^2} + \alpha_e^2 \tilde{\varphi}_e = 0, \quad \frac{d^2 \tilde{\psi}_e}{dx_3^2} + \beta_e^2 \tilde{\psi}_e = 0 \quad (12)$$

式中  $\alpha_e = \sqrt{\omega^2/v_p^2 - \xi^2}$ ,  $\beta_e = \sqrt{\omega^2/v_s^2 - \xi^2}$ ,故可得到单相弹性固体介质中位移势函数的通解为:

$$\tilde{\varphi}_e = A_{te} e^{-i\alpha_e x_3} + A_{re} e^{i\alpha_e x_3} \quad (13a)$$

$$\tilde{\psi}_e = B_{te} e^{-i\beta_e x_3} + B_{re} e^{i\beta_e x_3} \quad (13b)$$

式中  $A_{te}$ 和 $A_{re}$ 分别为单相固体介质中透射P波和反射P波的波幅, $B_{te}$ 和 $B_{re}$ 分别为单相固体介质中透射S波和反射S波的波幅。

### 2.2 非饱和多孔介质的解

将式(11)代入方程(10a),(10b)和(10c)中,经过Fourier变换整理可得:

$$\begin{aligned} (\mu_p + B_1) \frac{d^2 \tilde{\varphi}_s}{dx_3^2} + b_{11} \tilde{\varphi}_s + B_2 \frac{d^2 \tilde{\varphi}_1}{dx_3^2} + b_{12} \tilde{\varphi}_1 + \\ B_3 \frac{d^2 \tilde{\varphi}_g}{dx_3^2} + b_{13} \tilde{\varphi}_g = 0 \end{aligned} \quad (14a)$$

$$\begin{aligned} a_{11} \frac{d^2 \tilde{\varphi}_s}{dx_3^2} + b_{21} \tilde{\varphi}_s + a_{12} \frac{d^2 \tilde{\varphi}_1}{dx_3^2} + b_{22} \tilde{\varphi}_1 + a_{13} \frac{d^2 \tilde{\varphi}_g}{dx_3^2} + \\ b_{23} \tilde{\varphi}_g = 0 \end{aligned} \quad (14b)$$

$$\begin{aligned} a_{21} \frac{d^2 \tilde{\varphi}_s}{dx_3^2} + b_{31} \tilde{\varphi}_s + a_{22} \frac{d^2 \tilde{\varphi}_1}{dx_3^2} + b_{32} \tilde{\varphi}_1 + a_{23} \frac{d^2 \tilde{\varphi}_g}{dx_3^2} + \\ b_{33} \tilde{\varphi}_g = 0 \end{aligned} \quad (14c)$$

式中  $b_{11} = \bar{\rho}_s \omega^2 - (\mu_p + B_1) \xi^2$ ,  $b_{12} = \bar{\rho}_1 \omega^2 - B_2 \xi^2$ ,  $b_{13} = \bar{\rho}_g \omega^2 - B_3 \xi^2$ ,  $b_{21} = -C_1 - a_{11} \xi^2$ ,  $b_{22} = -C_2 - a_{12} \xi^2$ ,  $b_{23} = -a_{13} \xi^2$ ,  $b_{31} = -C_3 - a_{21} \xi^2$ ,  $b_{32} = -a_{22} \xi^2$ ,  $b_{33} = -C_4 - a_{23} \xi^2$ 。

设方程组(14)的解为:

$$[\tilde{\varphi}_s \quad \tilde{\varphi}_1 \quad \tilde{\varphi}_g]^T = [c^s \quad c^1 \quad c^g]^T \exp(\lambda x_3) \quad (15)$$

将式(15)代入式(14)得到线性方程组:

$$\begin{bmatrix} \lambda^2 B_3 + b_{13} & \lambda^2 B_2 + b_{12} & \lambda^2 (\mu_p + B_1) + b_{11} \\ \lambda^2 a_{13} + b_{23} & \lambda^2 a_{12} + b_{22} & \lambda^2 a_{11} + b_{21} \\ \lambda^2 a_{23} + b_{33} & \lambda^2 a_{22} + b_{32} & \lambda^2 a_{21} + b_{31} \end{bmatrix} \begin{bmatrix} c^g \\ c^1 \\ c^s \end{bmatrix} = 0 \quad (16)$$

式(16)有非零解的条件为系数矩阵行列式为0,即:

$$\beta_1 \lambda^6 + \beta_2 \lambda^4 + \beta_3 \lambda^2 + \beta_4 = 0 \quad (17)$$

设式(17)的根为 $\pm \lambda_n$  ( $n=1, 2, 3$ ),则 $\lambda_n$ 由下式给出:

$$\lambda_n = \sqrt{r_n} \quad (\text{Re}[\lambda_n] \geq 0, n=1, 2, 3) \quad (18)$$

式中  $\beta_n$  ( $n=1, 2, 3, 4$ )见附录A。

可得到常微分方程组(14)的解为:

$$\tilde{\varphi}_s = \sum_{n=1}^3 (A_{tpn} e^{-\lambda_n x_3} + A_{tpn} e^{\lambda_n x_3}) \quad (19a)$$

$$\tilde{\varphi}_1 = \sum_{n=1}^3 \delta_{pn}^1 (A_{tpn} e^{-\lambda_n x_3} + A_{tpn} e^{\lambda_n x_3}) \quad (19b)$$

$$\tilde{\varphi}_g = \sum_{n=1}^3 \delta_{pn}^g (A_{tpn} e^{-\lambda_n x_3} + A_{tpn} e^{\lambda_n x_3}) \quad (19c)$$

式中  $\delta_{pn}^1, \delta_{pn}^g$ 见附录A; $A_{tpn}$ 和 $A_{tpn}$  ( $n=1, 2, 3$ )分别为非饱和土多孔介质中透射 $P_1$ 波, $P_2$ 波, $P_3$ 波和反射 $P_1$ 波, $P_2$ 波, $P_3$ 波的波幅。

将式(11)代入方程(10d),(10e)和(10f)中,经过Fourier变换整理得:

$$\mu_p \frac{d^2 \tilde{\psi}_s}{dx_3^2} + d_{11} \tilde{\psi}_s + d_{12} \tilde{\psi}_1 + d_{13} \tilde{\psi}_g = 0 \quad (20a)$$

$$d_{21} \tilde{\psi}_s + d_{22} \tilde{\psi}_1 = 0 \quad (20b)$$

$$d_{31} \tilde{\psi}_s + d_{32} \tilde{\psi}_1 = 0 \quad (20c)$$

式中  $d_{11} = \bar{\rho}_s \omega^2 - \mu_p \xi^2$ ,  $d_{12} = \bar{\rho}_1 \omega^2$ ,  $d_{13} = \bar{\rho}_g \omega^2$ ,  $d_{21} = C_1$ ,  $d_{22} = C_2$ ,  $d_{31} = C_3$ ,  $d_{32} = C_4$ 。

设方程组(20)的解为:

$$[\tilde{\psi}_s \quad \tilde{\psi}_1 \quad \tilde{\psi}_g]^T = [d^s \quad d^1 \quad d^g]^T \exp(rx_3) \quad (21)$$

将式(21)代入式(20)得到线性方程组:

$$\begin{bmatrix} d_{13} & d_{12} & \mu_p r^2 + d_{11} \\ 0 & d_{22} & d_{21} \\ d_{33} & 0 & d_{31} \end{bmatrix} \begin{bmatrix} d^g \\ d^l \\ d^s \end{bmatrix} = 0 \quad (22)$$

式(22)有非零解的条件为系数矩阵行列式为0,即:

$$\beta_5 r^2 + \beta_6 = 0 \quad (23)$$

式(23)的根为±r,则r由下式给出:

$$r = \sqrt{-\beta_6/\beta_5} \quad (\text{Re}[r] \geq 0) \quad (24)$$

式中  $\beta_n (n=5, 6)$  见附录 A。

可得到常微分方程组(20)的解为:

$$\tilde{\psi}_s = B_{1s} e^{-rx_3} + B_{rs} e^{rx_3} \quad (25a)$$

$$\tilde{\psi}_l = \delta_s^l (B_{1s} e^{-rx_3} + B_{rs} e^{rx_3}) \quad (25b)$$

$$\tilde{\psi}_g = \delta_s^g (B_{1s} e^{-rx_3} + B_{rs} e^{rx_3}) \quad (25c)$$

式中  $\delta_s^l, \delta_s^g$  见附录 A;  $B_{1s}$  和  $B_{rs}$  分别为非饱和土多孔介质中透射 S 波和反射 S 波的波幅。

### 3 非饱和土地基动力响应求解

#### 3.1 地基动力响应

在直角坐标系中,各位移分量可用位移势函数  $\varphi$  和  $\psi$  表示为:

$$u_1 = \frac{\partial \varphi}{\partial x_1} - \frac{\partial \psi}{\partial x_3}, u_3 = \frac{\partial \varphi}{\partial x_3} + \frac{\partial \psi}{\partial x_1} \quad (26)$$

将式(13)和(26)代入式(2)和(3)中,将式(19), (25)和(26)代入式(6d), (6e), (7)和(9)中,可分别得到弹性介质和非饱和多孔介质在 Fourier 变换域中的位移和应力表达式。

在  $0 \leq x_3 \leq H$  的区域内:

$$\tilde{u}_1^{sl} = i\xi \sum_{n=1}^3 (A_{1pn}^l e^{-\lambda_n x_3} + A_{1pn}^l e^{\lambda_n x_3}) + r (B_{1s}^l e^{-rx_3} - B_{rs}^l e^{rx_3}) \quad (27a)$$

$$\tilde{u}_3^{sl} = \sum_{n=1}^3 [-\lambda_n (A_{1pn}^l e^{-\lambda_n x_3} - A_{1pn}^l e^{\lambda_n x_3})] + i\xi (B_{1s}^l e^{-rx_3} + B_{rs}^l e^{rx_3}) \quad (27b)$$

$$\tilde{u}_3^{ll} = \sum_{n=1}^3 [-\lambda_n \delta_{pn}^l (A_{1pn}^l e^{-\lambda_n x_3} - A_{1pn}^l e^{\lambda_n x_3})] + i\xi \delta_s^l (B_{1s}^l e^{-rx_3} + B_{rs}^l e^{rx_3}) \quad (27c)$$

$$\tilde{u}_3^{gl} = \sum_{n=1}^3 [-\lambda_n \delta_{pn}^g (A_{1pn}^l e^{-\lambda_n x_3} - A_{1pn}^l e^{\lambda_n x_3})] + i\xi \delta_s^g (B_{1s}^l e^{-rx_3} + B_{rs}^l e^{rx_3}) \quad (27d)$$

$$\tilde{\sigma}_{13}^l = 2\mu_p i\xi \sum_{n=1}^3 [-\lambda_n (A_{1pn}^l e^{-\lambda_n x_3} - A_{1pn}^l e^{\lambda_n x_3})] - \mu_p (r^2 + \xi^2) (B_{1s}^l e^{-rx_3} + B_{rs}^l e^{rx_3}) \quad (27e)$$

$$\tilde{\sigma}_{33}^l = \sum_{n=1}^3 [\chi_n (A_{1pn}^l e^{-\lambda_n x_3} + A_{1pn}^l e^{\lambda_n x_3})] - 2i\xi r \mu_p (B_{1s}^l e^{-rx_3} - B_{rs}^l e^{rx_3}) \quad (27f)$$

$$\tilde{p}^{ll} = \sum_{n=1}^3 (a_{11} + a_{12} \delta_{pn}^l + a_{13} \delta_{pn}^g) \cdot (\xi^2 - \lambda_n^2) (A_{1pn}^l e^{-\lambda_n x_3} + A_{1pn}^l e^{\lambda_n x_3}) \quad (27g)$$

$$\tilde{p}^{gl} = \sum_{n=1}^3 (a_{21} + a_{22} \delta_{pn}^l + a_{23} \delta_{pn}^g) \cdot (\xi^2 - \lambda_n^2) (A_{1pn}^l e^{-\lambda_n x_3} + A_{1pn}^l e^{\lambda_n x_3}) \quad (27h)$$

式中  $\chi_n = [a\gamma(a_{11} + a_{12} \delta_{pn}^l + a_{13} \delta_{pn}^g) + a(1 - \gamma)(a_{21} + a_{22} \delta_{pn}^l + a_{23} \delta_{pn}^g)](\lambda_n^2 - \xi^2) + [(\lambda_p + 2\mu_p)\lambda_n^2 - \lambda_p \xi^2]$ 。

在  $H \leq x_3 \leq H + h_w$  的区域内:

$$\tilde{u}_1^e = i\xi (A_{1te} e^{-i\alpha_e x_3} + A_{re} e^{i\alpha_e x_3}) + i\beta_e (B_{1e} e^{-i\beta_e x_3} - B_{re} e^{i\beta_e x_3}) \quad (28a)$$

$$\tilde{u}_3^e = -i\alpha_e (A_{1te} e^{-i\alpha_e x_3} - A_{re} e^{i\alpha_e x_3}) + i\xi (B_{1e} e^{-i\beta_e x_3} + B_{re} e^{i\beta_e x_3}) \quad (28b)$$

$$\tilde{\sigma}_{13}^e = 2\mu_e \xi \alpha_e (A_{1te} e^{-i\alpha_e x_3} - A_{re} e^{i\alpha_e x_3}) + \mu_e (\beta_e^2 - \xi^2) (B_{1e} e^{-i\beta_e x_3} + B_{re} e^{i\beta_e x_3}) \quad (28c)$$

$$\tilde{\sigma}_{33}^e = [-\lambda_e \xi^2 - \alpha_e^2 (\lambda_e + 2\mu_e)] (A_{1te} e^{-i\alpha_e x_3} + A_{re} e^{i\alpha_e x_3}) + 2\mu_e \beta_e \xi (B_{1e} e^{-i\beta_e x_3} - B_{re} e^{i\beta_e x_3}) \quad (28d)$$

如果波阻板为非饱和土多孔介质,则此区域内的式(28)将退化为式(27)。

在  $x_3 \geq H + h_w$  的区域内:

$$\tilde{u}_1^{sll} = i\xi \sum_{n=1}^3 (A_{1pn}^{ll} e^{-\lambda_n x_3}) + r B_{1s}^{ll} e^{-rx_3} \quad (29a)$$

$$\tilde{u}_3^{sll} = \sum_{n=1}^3 (-\lambda_n A_{1pn}^{ll} e^{-\lambda_n x_3}) + i\xi B_{1s}^{ll} e^{-rx_3} \quad (29b)$$

$$\tilde{u}_3^{lll} = \sum_{n=1}^3 (-\lambda_n \delta_{pn}^l A_{1pn}^{ll} e^{-\lambda_n x_3}) + i\xi \delta_s^l B_{1s}^{ll} e^{-rx_3} \quad (29c)$$

$$\tilde{u}_3^{gll} = \sum_{n=1}^3 (-\lambda_n \delta_{pn}^g A_{1pn}^{ll} e^{-\lambda_n x_3}) + i\xi \delta_s^g B_{1s}^{ll} e^{-rx_3} \quad (29d)$$

$$\tilde{\sigma}_{13}^{ll} = 2\mu_p i\xi \sum_{n=1}^3 (-\lambda_n A_{1pn}^{ll} e^{-\lambda_n x_3}) - \mu_p (r^2 + \xi^2) B_{1s}^{ll} e^{-rx_3} \quad (29e)$$

$$\tilde{\sigma}_{33}^{ll} = \sum_{n=1}^3 (\chi_n A_{1pn}^{ll} e^{-\lambda_n x_3}) - 2i\xi r \mu_p B_{1s}^{ll} e^{-rx_3} \quad (29f)$$

#### 3.2 边界条件及求解

对于荷载作用在半平面表面,考虑地表透气透水的边界条件以及各层面处的连续条件:

在  $x_3 = 0$  处:

$$\tilde{\sigma}_{33}^l = q_0 \frac{\sin(\xi l)}{\xi l}, \tilde{\sigma}_{13}^l = 0, \tilde{p}^{ll} = 0, \tilde{p}^{gl} = 0 \quad (30)$$

在  $x_3 = H$  处:

$$\tilde{\sigma}_{33}^l = \tilde{\sigma}_{33}^e, \tilde{\sigma}_{13}^l = \tilde{\sigma}_{13}^e, \tilde{u}_3^{sl} = \tilde{u}_3^e, \tilde{u}_1^{sl} = \tilde{u}_1^e, \tilde{u}_3^{ll} = \tilde{u}_3^e, \tilde{u}_3^{gl} = \tilde{u}_3^e \quad (31)$$

在  $x_3 = H + h_w$  处:

$$\tilde{\sigma}_{33}^e = \tilde{\sigma}_{33}^{ll}, \tilde{\sigma}_{13}^e = \tilde{\sigma}_{13}^{ll}, \tilde{u}_3^e = \tilde{u}_3^{sll}, \tilde{u}_1^e = \tilde{u}_1^{sll}$$

$$\tilde{u}_3^{\text{sl}} = \tilde{u}_3^{\text{ll}}, \tilde{u}_3^{\text{sl}} = \tilde{u}_3^{\text{ll}} \quad (32)$$

将式(27),(28)和(29)代入到边界条件式(30),(31)和(32)中,可以得到如下的矩阵方程组:

$$Tx = f \quad (33)$$

式中 矩阵  $T$  以及矢量  $x$  和  $f$  中的各元素详见附录 B。

通过求解方程组(33),获得  $x$  内各类波的波幅,结合式(27),(28)和(29)即可获得 Fourier 变换域内非饱和土地基和波阻板中任意点的应力和位移响应。

## 4 数值算例

对于非饱和土地基,由于饱和度的变化会引起土中剪切模量的改变,因此在本文中采用修正后的动剪切模量<sup>[23-24]</sup>公式:

$$\mu_p = \mu_s + \frac{2050}{\alpha} \ln \left[ \sqrt{S_e^{-2} - 1} + S_e^{-1} \right] \tan \phi' \quad (34)$$

为了研究波阻板对非饱和土地基振动的控制效果,本文选取一组非饱和土地基的物理力学参数<sup>[23]</sup>如表 1 所示。选取均质波阻板的物理力学参数如下:弹性模量  $E_c = 6.5 \times 10^8$  Pa,泊松比  $\nu = 0.3$ ,密度  $\rho_c = 2458$  kg/m<sup>3</sup>,取荷载幅值  $q_0 = 1$  kPa,分布长度  $l = 1$  m。由于被积函数表达式较为复杂,因此很难得到 Fourier 逆变换的封闭形式解,本文采用 FFT 方法完成 Fourier 逆变换,波数的离散点为 1024,空间计算区间为 100 m。

表 1 非饱和土的物理力学参数<sup>[23]</sup>

Tab. 1 Physical and mechanical parameters of unsaturated soils

参数	数值	参数	数值	参数	数值
$K_g/\text{kPa}$	100	$K_s/\text{GPa}$	36	$S_r$	0.1~1
$\rho_g/(\text{kg}\cdot\text{m}^{-3})$	1.29	$\rho_s/(\text{kg}\cdot\text{m}^{-3})$	2700	$d$	2
$\eta_g/(\text{N}\cdot\text{s}\cdot\text{m}^{-2})$	$1.5 \times 10^5$	$\phi'/(^{\circ})$	21	$S_{w0}$	0.05
$K_l/\text{GPa}$	2.1	$\nu$	0.2	$k/\text{m}^2$	$1 \times 10^{12}$
$\rho_l/(\text{kg}\cdot\text{m}^{-3})$	1000	$\mu_s/\text{MPa}$	19.4	$\alpha/\text{Pa}^{-1}$	$1 \times 10^4$
$\eta_l/(\text{N}\cdot\text{s}\cdot\text{m}^{-2})$	0.001	$n$	0.6	$m$	0.5

为了分析非饱和土地基与饱和土地基中波阻板隔振效果的区别,考虑上覆土层厚度  $H = 2$  m,波阻板厚度  $h_w = 2$  m,波阻板弹性模量  $E_c = 6.5 \times 10^8$  Pa,荷载频率  $\omega = 1$  rad/s 的情形下,本文将非饱和土地基退化到饱和土地基,非饱和土地基中考虑饱和度  $S_r = 0.8$ ,图 2,3 分别给出了两种地基类型下地表竖向位移和水平位移沿水平方向变化的曲线。从图 2,3 中可以看出,波阻板设置在非饱和土地基中的地表位移幅值比在饱和土地基中更小,说明在实际工程进行波阻

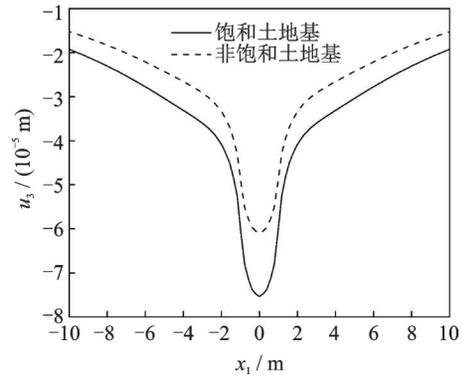


图 2 地表竖向位移变化曲线

Fig. 2 Variations of vertical displacement at the ground surface

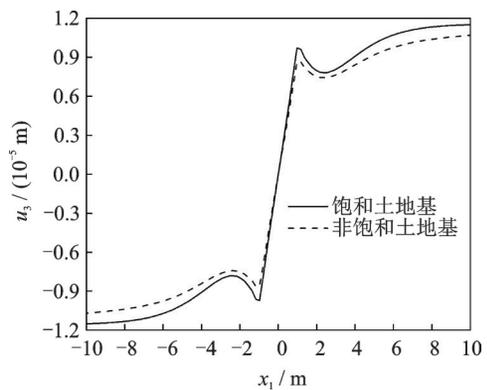


图 3 地表水平位移变化曲线

Fig. 3 Variations of horizontal displacement at the ground surface

板隔振设计时要选择与实际场地相符的地基模型,把场地土视为饱和土地基从而没有考虑土体饱和度对隔振效果的影响,这与实际现象是有差别的。

为了说明非饱和土地基中设置波阻板的隔振作用以及饱和度  $S_r$  对其隔振效果的影响,考虑上覆土层厚度  $H = 2$  m,波阻板厚度  $h_w = 2$  m,  $E_c = 6.5 \times 10^8$  Pa,  $\omega = 1$  rad/s 时,图 4,5 分别绘出了土体饱和度  $S_r$  从 0.3, 0.5, 0.7, 0.9 逐渐增大时分别考虑是否设置波阻板时地表竖向位移和水平位移沿水平方向变化的曲线。从图 4 和 5 中可以看出,非饱和土地基中水平位移和竖向位移的振动相位因为波阻板的设置而发生改变,在相同  $S_r$  下波阻板隔振屏障的存在均使得竖向位移和水平位移幅值显著降低,故非饱和土地基中设置波阻板能够取得很好的隔振效果。另外,随着土体  $S_r$  的增大,地表竖向和水平位移幅值随之增大。说明非饱和土地基中波阻板隔振效果受饱和度的影响明显,非饱和土地基中波阻板隔振效果随着饱和度的增大而降低。

为了分析波阻板的埋深对地基隔振效果的影响,图 6 和 7 分别绘出了在  $S_r = 0.8$ ,  $h_w = 2$  m,  $E_c = 6.5 \times 10^8$  Pa,  $\omega = 1$  rad/s,波阻板埋深从 1, 2, 3, 4 m

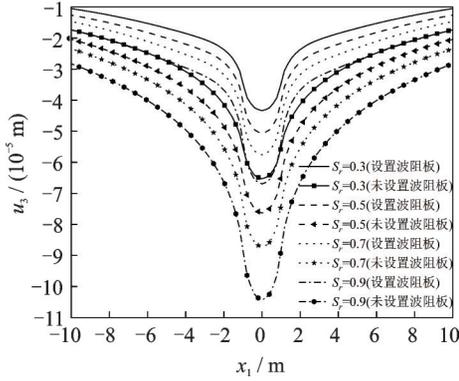


图 4 地表竖向位移随饱和度的变化曲线

Fig. 4 Variations of vertical displacement at the ground surface with saturation

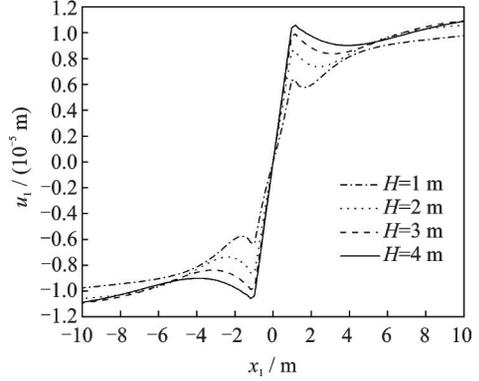


图 7 地基表面水平位移变化曲线

Fig. 7 Variations of horizontal displacement at the ground surface

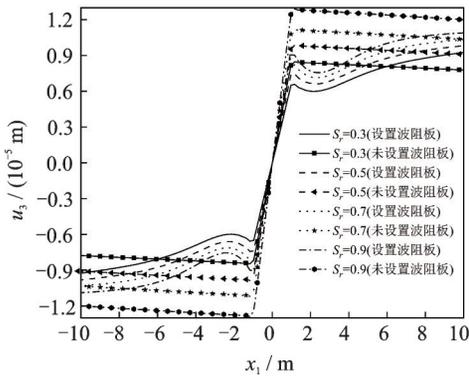


图 5 地表水平位移随饱和度的变化曲线

Fig. 5 Variations of horizontal displacement at the ground surface with saturation

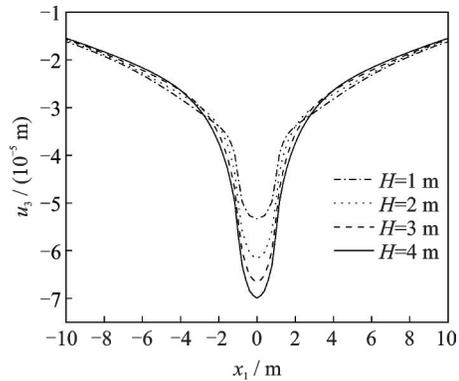


图 6 地基表面竖向位移变化曲线

Fig. 6 Variations of vertical displacement at the ground surface

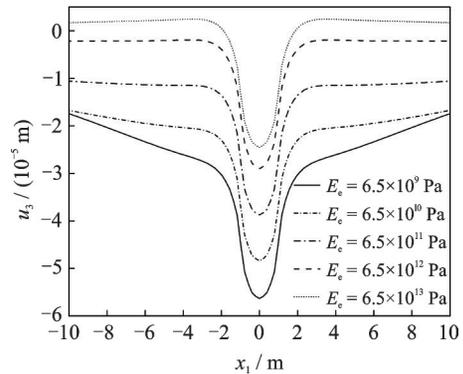


图 8 地基表面竖向位移变化曲线

Fig. 8 Variations of vertical displacement at the ground surface

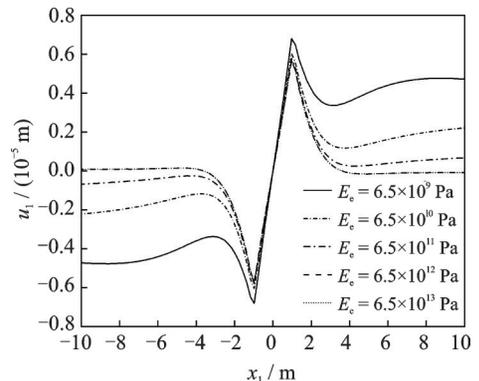


图 9 地基表面水平位移变化曲线

Fig. 9 Variations of horizontal displacement at the ground surface

为了分析波阻板的弹性模量对地基隔振效果的影响,图8和9分别绘出了  $S_r=0.8, H=2\text{ m}, h_w=2\text{ m}, \omega=1\text{ rad/s}$ ,波阻板的弹性模量  $E_e$  在  $6.5 \times 10^9 \sim 6.5 \times 10^{13}\text{ Pa}$  范围内逐渐增大时,地基表面竖向位移和水平位移沿水平方向的变化曲线。根据图8和9可知,随着弹性模量的增高,地基表面位移随之明显降低,说明增加波阻板弹性模量是增大其隔振效果的一种有效措施。其中当  $E_e \geq 6.5 \times 10^{12}\text{ Pa}$  时,地表位移幅值随着弹性模量的继续增大虽然也随之降低,但

逐渐增大时,地基表面竖向位移和水平位移沿水平方向的变化曲线。由图6,7可以看出随着波阻板埋置深度的不断增大,地表竖向位移和水平位移幅值随之显著增大。非饱和土地基中波阻板埋深对其隔振效果的影响与文献[16]中波阻板埋深不同时位移变化规律表现相似。这是因为波阻板是利用地基存在截止频率的原理隔振,而截止频率的大小与上覆土层的厚度,即与波阻板的埋深成反比<sup>[16,19,25]</sup>。因此,在实际的非饱和土地基中,波阻板埋深越浅隔振效果越好。

其降低幅度逐渐减小,说明当弹性模量增大到一定程度后,其对波阻板隔振效果的作用将不再明显。

为了分析波阻板的厚度对地基隔振效果的影响,图 10,11 分别绘出了在  $S_r=0.8, H=2\text{ m}, E_c=6.5 \times 10^8\text{ Pa}, \omega=1\text{ rad/s}$ , 波阻板厚度  $h_w$  从 1, 2, 3, 4 m 逐渐增大时,地基表面竖向位移和水平位移沿水平方向的变化曲线。从图 10,11 可以看出,随着波阻板的厚度不断增加,地表竖向位移和水平位移随之显著减小。当波阻板厚度  $h_w \geq 3\text{ m}$  时,随着波阻板厚度的增大,地表位移幅值仍然随之减小,但是位移幅值降低的幅度却逐渐减小。考虑到适宜的经济成本且起到较好的隔振效果,波阻板的厚度不宜设置过厚。

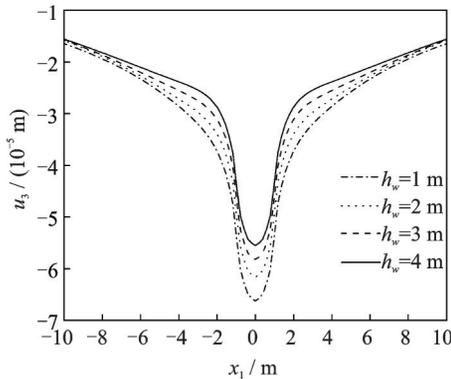


图 10 地基表面竖向位移变化曲线

Fig. 10 Variations of vertical displacement at the ground surface

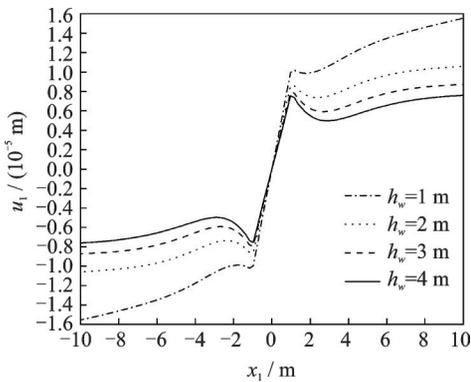


图 11 地基表面水平位移变化曲线

Fig. 11 Variations of horizontal displacement at the ground surface

为了分析荷载频率对波阻板隔振效果的影响,图 12,13 分别绘出了在  $S_r=0.8, H=2\text{ m}, h_w=2\text{ m}, E_c=6.5 \times 10^8\text{ Pa}$ , 荷载频率  $\omega$  从 1, 10, 30, 50 rad/s 逐渐增大时地基表面竖向位移和水平位移沿水平方向的变化曲线。从图 12,13 可以看出随着荷载频率的不断增大,地表竖向位移和水平位移均随之减小。当荷载频率继续增加时,位移幅值仍然随之减小,但减小的不再明显,说明波阻

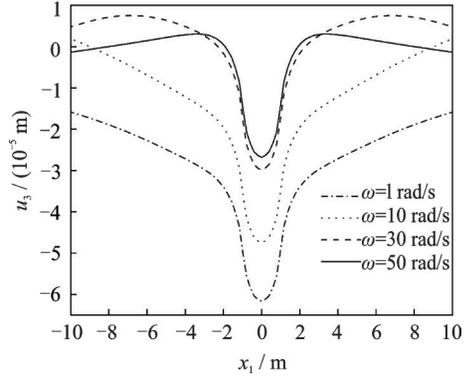


图 12 地基表面竖向位移变化曲线

Fig. 12 Variations of vertical displacement at the ground surface

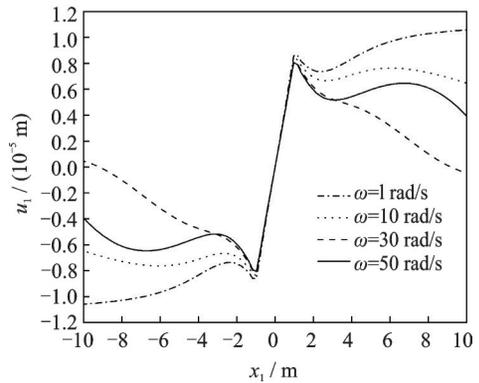


图 13 地基表面水平位移变化曲线

Fig. 13 Variations of horizontal displacement at the ground surface

板在较高荷载频率作用下可以起到更好的隔振效果。

### 5 结 论

(1)非饱和土地基中设置单相固体波阻板能够取得很好的隔振效果。饱和度对地基中波阻板的隔振效果影响显著,在实际工程进行波阻板隔振设计时要选择与实际场地相符的地基模型。

(2)非饱和土地基中波阻板隔振效果随埋深和饱和度的增大而降低,特别是埋深对其隔振效果影响非常显著。

(3)非饱和土地基中波阻板隔振效果随着荷载频率、波阻板厚度和弹性模量的增加而提高,但当厚度和弹性模量增大到一定程度后其对隔振效果作用不再明显。

### 参考文献:

[1] Woods R D. Screening of surface waves in soils [J]. Journal of the Soil Mechanics and Foundations Division, ASCE, 1968, 94 (4): 951-979.

[2] With C, Bahrekazemi M, Bodare A. Wave barrier of lime-cement columns against train-induced ground-

- borne vibrations[J]. *Soil Dynamics and Earthquake Engineering*, 2009, 29(6): 1027-1033.
- [3] Katsuya I, Ryota S, Tomihiro H, et al. Systematic analyses of vibration noise of a vibration isolation system for high-resolution scanning tunneling microscopes [J]. *Review of Scientific Instruments*, 2011, 82(8): 083702.
- [4] 徐平,周新民,夏唐代.应用屏障进行被动隔振的研究综述[J].*地震工程学报*, 2015, 37(1): 88-93.  
Xu Ping, Zhou Xinmin, Xia Tangdai. Review on passive vibration isolation using barriers [J]. *China Earthquake Engineering Journal*, 2015, 37(1): 88-93.
- [5] 巴振宁,王靖雅,梁建文.层状地基中隔振沟对移动列车荷载隔振研究-2.5维IBEM方法[J].*振动工程学报*, 2016, 29(5): 860-873.  
Ba Zhenning, Wang Jingya, Liang Jianwen. Reduction of train-induced vibrations by using a trench in a layered foundation [J]. *Journal of Vibration Engineering*, 2016, 29(5): 860-873.
- [6] 刘中宪,王少杰.非连续群桩屏障对平面P、SV波的隔离效应:二维宽频带间接边界积分方程法模拟[J].*岩土力学*, 2016, 37(4): 1195-1207.  
Liu Zhongxian, Wang Shaojie. Isolation effect of discontinuous pile-group barriers on plane P and SV waves: Simulation based on 2D broadband indirect boundary integration equation method [J]. *Rock and Soil Mechanics*, 2016, 37(4): 1195-1207.
- [7] Gao G Y, Zhang Q W, Chen J, et al. Field experiments and numerical analysis on the ground vibration isolation of wave impeding block under horizontal and rocking coupled excitations [J]. *Soil Dynamics and Earthquake Engineering*, 2018, 115: 507-512.
- [8] 巴振宁,刘世朋,吴孟桃,等.周期分布桩体对平面SH波隔振效应的解析求解[J].*岩土力学*, 2020, 41(9): 2861-2868.  
Ba Zhenning, Liu Shipeng, Wu Mengtao, et al. Analytical solution for isolation effect of plane SH waves by periodically distributed piles [J]. *Rock and Soil Mechanics*, 2020, 41(9): 2861-2868.
- [9] 巴振宁,刘世朋,吴孟桃,等.周期分布群桩屏障对平面弹性波隔振效应的解析求解[J].*岩石力学与工程学报*, 2020, 39(7): 1468-1482.  
Ba Zhenning, Liu Shipeng, Wu Mengtao, et al. Analytical solution for isolation effect of periodically distributed pile-group barriers against plane elastic wave [J]. *Chinese Journal of Rock Mechanics and Engineering*, 2020, 39(7): 1468-1482.
- [10] 巴振宁,刘世朋,吴孟桃,等.饱和土中周期排列管桩对平面SV波隔振的解析求解[J].*岩土力学*, 2021, 42(3): 627-637.  
Ba Zhenning, Liu Shipeng, Wu Mengtao, et al. Analytical solution for isolation effect of plane SV waves by pipe piles with periodic arrangement in saturated soil [J]. *Rock and Soil Mechanics*, 2021, 42(3): 627-637.
- [11] 舒进辉,马强,周凤玺,等.非饱和土地基中P<sub>1</sub>波通过波阻板的特性研究[J].*岩土力学*, 2022, 43(4): 1-13.  
Shu Jinhui, Ma Qiang, Zhou Fengxi, et al. Propagation characteristics of P<sub>1</sub> wave passing through wave impeding block in unsaturated soil [J]. *Rock and Soil Mechanics*, 2022, 43(4): 1-13.
- [12] 高广运.非连续屏障地面隔振理论与应用[D].杭州:浙江大学,1998.  
Gao Guangyun. Theory and application of ground vibration isolation by discontinuous barrier [D]. Hangzhou: Zhejiang University, 1998.
- [13] Chou N, Le R, Schmid G. An approach to reduce foundation vibrations and soil waves using dynamic transmitting behavior of a soil layer [J]. *Bauingenieur*, 1991, 66: 215-221.
- [14] Takemiya H, Fujiwara A. Wave propagation/impediment in a stratum and wave impeding block (WIB) measured for SSI response reduction [J]. *Soil Dynamics and Earthquake Engineering*, 1994, 13(1): 49-61.
- [15] 周凤玺,马强,赖远明.含液饱和多孔波阻板的地基振动控制研究[J].*振动与冲击*, 2016, 35(1): 96-105.  
Zhou Fengxi, Ma Qiang, Lai Yuanming. Ground vibration control with fluid-saturated porous wave impeding blocks [J]. *Journal of Vibration and Shock*, 2016, 35(1): 96-105.
- [16] 马强,周凤玺,刘杰.梯度波阻板的地基振动控制研究[J].*力学学报*, 2017, 49(6): 1360-1369.  
Ma Qiang, Zhou Fengxi, Liu Jie. Analysis of ground vibration control by graded wave impeding block [J]. *Chinese Journal of Theoretical and Applied Mechanics*, 2017, 49(6): 1360-1369.
- [17] 田抒平,高盟,王滢,等. Duxseal隔振性能数值分析与现场试验研究[J].*岩土力学*, 2020, 41(5): 1770-1780.  
Tian Shuping, Gao Meng, Wang Ying, et al. Numerical analysis and field experiment of vibration isolation for Duxseal [J]. *Rock and Soil Mechanics*, 2020, 41(5): 1770-1780.
- [18] 高盟,张致松,王崇革,等.竖向激振力下WIB-Duxseal联合隔振试验研究[J].*岩土力学*, 2021, 42(2): 537-546.  
Gao Meng, Zhang Zhisong, Wang Chongge, et al. Field test on vibration isolation performance by WIB-Duxseal under vertical excitation [J]. *Rock and Soil Mechanics*, 2021, 42(2): 537-546.
- [19] 高广运,何俊锋,李宁,等.饱和地基上列车运行引起的地面振动隔振分析[J].*岩土力学*, 2011, 32(7): 2191-2198.  
Gao Guangyun, He Junfeng, Li Ning, et al. Analysis of isolating ground vibration induced by trains running on saturated ground [J]. *Rock and Soil Mechanics*,

- 2011, 32(7): 2191-2198.
- [20] 高广运, 王非, 陈功奇. 轨道交通荷载下饱和地基中波阻板主动隔振研究[J]. 振动工程学报, 2014, 27(3): 433-440.
- Gao Guangyun, Wang Fei, Chen Gongqi. Active vibration isolation of the saturated ground with wave impedance block inside and under the load of the travelling train [J]. Journal of Vibration Engineering, 2014, 27(3): 433-440.
- [21] Gao G Y, Chen J, Gu X Q, et al. Numerical study on the active vibration isolation by wave impeding block in saturated soils under vertical loading[J]. Soil Dynamics and Earthquake Engineering, 2017, 93: 99-112.
- [22] 徐长节, 丁海滨, 童立红, 等. 饱和土中夹水混凝土复合式隔振屏障的隔振分析[J]. 振动与冲击, 2019, 38(1): 251-257.
- Xu Changjie, Ding Haibin, Tong Lihong, et al. Vibration isolation analysis for concrete-water-concrete composite vibration isolation barriers in saturated soil [J]. Journal of Vibration and Shock, 2019, 38(1): 251-257.
- [23] 徐明江, 魏德敏. 非饱和土地基的三维非轴对称动力响应[J]. 工程力学, 2011, 28(3): 78-85.
- Xu Mingjiang, Wei Demin. 3D non-axisymmetrical dynamic response of unsaturated soils[J]. Engineering Mechanics, 2011, 28(3): 78-85.
- [24] Lu Z, Fang R, Yao H L. Dynamic responses of unsaturated half-space soil to a moving harmonic rectangular load[J]. International Journal for Numerical and Analytical Methods in Geomechanics, 2018, 42(9): 1057-1077.
- [25] 高广运, 李伟. 二维地基波阻板隔振分析[J]. 地震工程与工程振动, 2005, 24(2): 130-135.
- Gao Guangyun, Li Wei. 2-D analysis of ground vibration isolation using wave impeding block [J]. Earthquake Engineering and Engineering Vibration, 2005, 24(2): 130-135.

## Study on vibration isolation effect of wave impeding block in unsaturated soil foundation under a harmonic load

ZHANG Meng<sup>1</sup>, MA Qiang<sup>1,2</sup>

(1.School of Civil Engineering, Qinghai University, Xining 810016, China;

2.Qinghai Provincial Key Laboratory of Energy-saving Building Materials and Engineering Safety, Xining 810016, China)

**Abstract:** In view of the universality and complexity of unsaturated soil foundation vibration, the control of environmental vibration of ground vibration control of unsaturated soil foundation has become a research focus in soil dynamics. Based on the theory of single phase elastic media and porous mixture media, the vibration isolation effect of single phase elastic wave impeding block in an unsaturated soil foundation under harmonic load is studied. Considering the boundary conditions of surface drainage and exhaust, using the Fourier transform and Helmholtz vector decomposition principle, the calculation formula for the dynamic response of the ground under dynamic loads is established. The effects of soil saturation, load frequency, embedded depth, thickness and elastic modulus of wave impeding block on the vibration isolation performance of unsaturated soil foundation is addressed. The results show that the wave impeding block in unsaturated ground can achieve a good vibration isolation effect. The surface displacement amplitude decreases significantly with the decrease of the saturation and the embedded depth of the wave impeding block, and decreases significantly with the increase of the load frequency, the thickness and the elastic modulus of the wave impeding block.

**Key words:** unsaturated soil ground; wave impeding block; vibration isolation effectiveness; dynamic response

作者简介: 张 猛(1998—),男,硕士研究生。E-mail:15133839505@163.com。

通讯作者: 马 强(1990—),男,博士,副教授。E-mail:maqiang0104@163.com。

### 附录 A

$$\delta_{pn}^1 = -\frac{(B_1 a_{13} - B_3 a_{11} + a_{13} \mu_p) r_n^2 + (B_1 b_{23} - B_3 b_{21} - a_{11} b_{13} + a_{13} b_{11} + b_{23} \mu_p) r_n + b_{11} b_{23} - b_{13} b_{21}}{(B_2 a_{13} - B_3 a_{12}) r_n^2 + (B_2 b_{23} - B_3 b_{22} - a_{12} b_{13} + a_{13} b_{12}) r_n + b_{12} b_{23} - b_{13} b_{22}},$$

$$\delta_{pn}^g = \frac{(B_1 a_{12} - B_2 a_{11} + a_{12} \mu_p) r_n^2 + (B_1 b_{22} - B_2 b_{21} - a_{11} b_{12} + a_{12} b_{11} + b_{22} \mu_p) r_n + b_{11} b_{22} - b_{12} b_{21}}{(B_2 a_{13} - B_3 a_{12}) r_n^2 + (B_2 b_{23} - B_3 b_{22} - a_{12} b_{13} + a_{13} b_{12}) r_n + b_{12} b_{23} - b_{13} b_{22}},$$

$$\delta_s^1 = -\frac{d_{21}}{d_{22}}, \quad \delta_s^g = \frac{d_{12} d_{21} - (\mu_p r^2 + d_{11}) d_{22}}{d_{13} d_{22}},$$

$$\begin{aligned}
\beta_1 &= -B_1 a_{12} a_{23} + B_1 a_{13} a_{22} + B_2 a_{11} a_{23} - B_2 a_{13} a_{21} - B_3 a_{11} a_{22} + B_3 a_{12} a_{21} - \mu_p a_{12} a_{23} + \mu_p a_{13} a_{22}, \\
\beta_2 &= -B_1 a_{12} b_{33} + B_1 a_{13} b_{32} + B_1 a_{22} b_{23} - B_1 a_{23} b_{22} + B_2 a_{11} b_{33} - B_2 a_{13} b_{31} - \\
&\quad B_2 a_{21} b_{23} + B_2 a_{23} b_{21} - B_3 a_{11} b_{32} + B_3 a_{12} b_{31} + B_3 a_{21} b_{22} - B_3 a_{22} b_{21} - \\
&\quad a_{11} a_{22} b_{13} + a_{11} a_{23} b_{12} + a_{12} a_{21} b_{13} - a_{12} a_{23} b_{11} - a_{13} a_{21} b_{12} + a_{13} a_{22} b_{11} - \\
&\quad \mu_p a_{12} b_{33} + \mu_p a_{13} b_{32} + \mu_p a_{22} b_{23} - \mu_p a_{23} b_{22}, \\
\beta_3 &= -B_1 b_{22} b_{33} + B_1 b_{23} b_{32} + B_2 b_{21} b_{33} - B_2 b_{23} b_{31} - B_3 b_{21} b_{32} + B_3 b_{22} b_{31} + \\
&\quad a_{11} b_{12} b_{33} - a_{11} b_{13} b_{32} - a_{12} b_{11} b_{33} + a_{12} b_{13} b_{31} + a_{13} b_{11} b_{32} - a_{13} b_{12} b_{31} - \\
&\quad a_{21} b_{12} b_{23} + a_{21} b_{13} b_{22} + a_{22} b_{11} b_{23} - a_{22} b_{13} b_{21} - a_{23} b_{11} b_{22} + a_{23} b_{12} b_{21} - \mu_p b_{22} b_{33} + \mu_p b_{23} b_{32}, \\
\beta_4 &= -b_{11} b_{22} b_{33} + b_{11} b_{23} b_{32} + b_{12} b_{21} b_{33} - b_{12} b_{23} b_{31} - b_{13} b_{21} b_{32} + b_{13} b_{22} b_{31}, \\
\beta_5 &= -\mu_p d_{22} d_{33}, \beta_6 = -d_{11} d_{22} d_{33} + d_{21} d_{12} d_{33} + d_{13} d_{22} d_{31}.
\end{aligned}$$

## 附录 B

方程组 (33) 的表达式为:

$$\begin{aligned}
& T_{16 \times 16} [A_{tp1}^I \ A_{tp2}^I \ A_{tp3}^I \ A_{tp1}^{II} \ A_{tp2}^{II} \ A_{tp3}^{II} \ B_{ts}^I \ B_{rs}^I \\
& A_{te} \ A_{re} \ B_{te} \ B_{re} \ A_{tp1}^{II} \ A_{tp2}^{II} \ A_{tp3}^{II} \ B_{ts}^{II}]^T = \\
& [q_0 \frac{\sin(\xi l)}{\xi l} \ 0 \ 0 \ 0 \ 0 \ 0 \ 0 \ 0 \ 0 \ 0 \ 0 \ 0 \ 0 \ 0 \ 0 \ 0]^T
\end{aligned}$$

矩阵  $T$  中非零元素为:

$$\begin{aligned}
T_{0101} &= T_{0104} = \chi_1, T_{0102} = T_{0105} = \chi_2, T_{0103} = T_{0106} = \chi_3, T_{0107} = -2\mu_p i \xi r, T_{0108} = 2\mu_p i \xi r, T_{0201} = -2\mu_p i \xi \lambda_1, \\
T_{0202} &= -2\mu_p i \xi \lambda_2, T_{0203} = -2\mu_p i \xi \lambda_3, T_{0204} = 2\mu_p i \xi \lambda_1, T_{0205} = 2\mu_p i \xi \lambda_2, T_{0206} = 2\mu_p i \xi \lambda_3, T_{0207} = T_{0208} = -\mu_p (r^2 + \xi^2), \\
T_{0301} &= T_{0304} = (a_{11} + a_{12} \delta_{p1}^1 + a_{13} \delta_{p1}^g) (\xi^2 - \lambda_1^2), T_{0302} = T_{0305} = (a_{11} + a_{12} \delta_{p2}^1 + a_{13} \delta_{p2}^g) (\xi^2 - \lambda_2^2), \\
T_{0303} &= T_{0306} = (a_{11} + a_{12} \delta_{p3}^1 + a_{13} \delta_{p3}^g) (\xi^2 - \lambda_3^2), T_{0401} = T_{0404} = (a_{21} + a_{22} \delta_{p1}^1 + a_{23} \delta_{p1}^g) (\xi^2 - \lambda_1^2), \\
T_{0402} &= T_{0405} = (a_{21} + a_{22} \delta_{p2}^1 + a_{23} \delta_{p2}^g) (\xi^2 - \lambda_2^2), T_{0403} = T_{0406} = (a_{21} + a_{22} \delta_{p3}^1 + a_{23} \delta_{p3}^g) (\xi^2 - \lambda_3^2), \\
T_{0501} &= \chi_1 e^{-\lambda_1 H}, T_{0502} = \chi_2 e^{-\lambda_2 H}, T_{0503} = \chi_3 e^{-\lambda_3 H}, T_{0504} = \chi_1 e^{\lambda_1 H}, T_{0505} = \chi_2 e^{\lambda_2 H}, T_{0506} = \chi_3 e^{\lambda_3 H}, T_{0507} = -2\mu_p i \xi r e^{-rH}, \\
T_{0508} &= 2\mu_p i \xi r e^{rH}, T_{0509} = [\lambda_e \xi^2 + \alpha_e^2 (\lambda_e + 2\mu_e)] e^{-i\alpha_e H}, T_{0510} = [\lambda_e \xi^2 + \alpha_e^2 (\lambda_e + 2\mu_e)] e^{i\alpha_e H}, T_{0511} = -2\mu_e \xi \beta_e e^{-i\beta_e H}, \\
T_{0512} &= 2\mu_e \xi \beta_e e^{i\beta_e H}, T_{0601} = -2\mu_p i \xi \lambda_1 e^{-\lambda_1 H}, T_{0602} = -2\mu_p i \xi \lambda_2 e^{-\lambda_2 H}, T_{0603} = -2\mu_p i \xi \lambda_3 e^{-\lambda_3 H}, T_{0604} = 2\mu_p i \xi \lambda_1 e^{\lambda_1 H}, \\
T_{0605} &= 2\mu_p i \xi \lambda_2 e^{\lambda_2 H}, T_{0606} = 2\mu_p i \xi \lambda_3 e^{\lambda_3 H}, T_{0607} = -\mu_p (r^2 + \xi^2) e^{-rH}, T_{0608} = -\mu_p (r^2 + \xi^2) e^{rH}, \\
T_{0609} &= -2\mu_p \xi \alpha_e e^{-i\alpha_e H}, T_{0610} = 2\mu_e \xi \alpha_e e^{i\alpha_e H}, T_{0611} = \mu_e (\xi^2 - \beta_e^2) e^{-i\beta_e H}, T_{0612} = \mu_e (\xi^2 - \beta_e^2) e^{i\beta_e H}, \\
T_{0701} &= -\lambda_1 e^{-\lambda_1 H}, T_{0702} = -\lambda_2 e^{-\lambda_2 H}, T_{0703} = -\lambda_3 e^{-\lambda_3 H}, T_{0704} = \lambda_1 e^{\lambda_1 H}, T_{0705} = \lambda_2 e^{\lambda_2 H}, T_{0706} = \lambda_3 e^{\lambda_3 H}, \\
T_{0707} &= i \xi e^{-rH}, T_{0708} = i \xi e^{rH}, T_{0709} = i \alpha_e e^{-i\alpha_e H}, T_{0710} = -i \alpha_e e^{i\alpha_e H}, T_{0711} = -i \xi e^{-i\beta_e H}, T_{0712} = -i \xi e^{i\beta_e H}, \\
T_{0801} &= i \xi e^{-\lambda_1 H}, T_{0802} = i \xi e^{-\lambda_2 H}, T_{0803} = i \xi e^{-\lambda_3 H}, T_{0804} = i \xi e^{\lambda_1 H}, T_{0805} = i \xi e^{\lambda_2 H}, T_{0806} = i \xi e^{\lambda_3 H}, T_{0807} = r e^{-rH}, \\
T_{0808} &= -r e^{rH}, T_{0809} = -i \xi e^{-i\alpha_e H}, T_{0810} = -i \xi e^{i\alpha_e H}, T_{0811} = -i \beta_e e^{-i\beta_e H}, T_{0812} = i \beta_e e^{i\beta_e H}, T_{0901} = \lambda_1 e^{-\lambda_1 H} (1 - \delta_{p1}^1), \\
T_{0902} &= \lambda_2 e^{-\lambda_2 H} (1 - \delta_{p2}^1), T_{0903} = \lambda_3 e^{-\lambda_3 H} (1 - \delta_{p3}^1), T_{0904} = \lambda_1 e^{\lambda_1 H} (\delta_{p1}^1 - 1), T_{0905} = \lambda_2 e^{\lambda_2 H} (\delta_{p2}^1 - 1), \\
T_{0906} &= \lambda_3 e^{\lambda_3 H} (\delta_{p3}^1 - 1), T_{0907} = i \xi e^{-rH} (\delta_s^1 - 1), T_{0908} = i \xi e^{rH} (\delta_s^1 - 1), T_{1001} = \lambda_1 e^{-\lambda_1 H} (1 - \delta_{p1}^g), \\
T_{1002} &= \lambda_2 e^{-\lambda_2 H} (1 - \delta_{p2}^g), T_{1003} = \lambda_3 e^{-\lambda_3 H} (1 - \delta_{p3}^g), T_{1004} = \lambda_1 e^{\lambda_1 H} (\delta_{p1}^g - 1), T_{1005} = \lambda_2 e^{\lambda_2 H} (\delta_{p2}^g - 1), \\
T_{1006} &= \lambda_3 e^{\lambda_3 H} (\delta_{p3}^g - 1), T_{1007} = i \xi e^{-rH} (\delta_s^g - 1), T_{1008} = i \xi e^{rH} (\delta_s^g - 1), T_{1109} = -[\lambda_e \xi^2 + \alpha_e^2 (\lambda_e + 2\mu_e)] e^{-i\alpha_e (H+h_w)}, \\
T_{1110} &= -[\lambda_e \xi^2 + \alpha_e^2 (\lambda_e + 2\mu_e)] e^{i\alpha_e (H+h_w)}, T_{1111} = 2\mu_e \xi \beta_e e^{-i\beta_e (H+h_w)}, T_{1112} = -2\mu_e \xi \beta_e e^{i\beta_e (H+h_w)}, \\
T_{1113} &= -\chi_1 e^{-\lambda_1 (H+h_w)}, T_{1114} = -\chi_2 e^{-\lambda_2 (H+h_w)}, T_{1115} = -\chi_3 e^{-\lambda_3 (H+h_w)}, T_{1116} = 2\mu_p i \xi r e^{-r(H+h_w)}, \\
T_{1209} &= 2\mu_e \xi \alpha_e e^{-i\alpha_e (H+h_w)}, T_{1210} = -2\mu_e \xi \alpha_e e^{i\alpha_e (H+h_w)}, T_{1211} = \mu_e (\beta_e^2 - \xi^2) e^{-i\beta_e (H+h_w)}, T_{1212} = \mu_e (\beta_e^2 - \xi^2) e^{i\beta_e (H+h_w)}, \\
T_{1213} &= 2\mu_p i \xi \lambda_1 e^{-\lambda_1 (H+h_w)}, T_{1214} = 2\mu_p i \xi \lambda_2 e^{-\lambda_2 (H+h_w)}, T_{1215} = 2\mu_p i \xi \lambda_3 e^{-\lambda_3 (H+h_w)}, T_{1216} = \mu_p (r^2 + \xi^2) e^{-r(H+h_w)}, \\
T_{1309} &= -i \alpha_e e^{-i\alpha_e (H+h_w)}, T_{1310} = i \alpha_e e^{i\alpha_e (H+h_w)}, T_{1311} = i \xi e^{-i\beta_e (H+h_w)}, T_{1312} = i \xi e^{i\beta_e (H+h_w)}, T_{1313} = \lambda_1 e^{-\lambda_1 (H+h_w)}, \\
T_{1314} &= \lambda_2 e^{-\lambda_2 (H+h_w)}, T_{1315} = \lambda_3 e^{-\lambda_3 (H+h_w)}, T_{1316} = -i \xi e^{-r(H+h_w)}, T_{1409} = i \xi e^{-i\alpha_e (H+h_w)}, T_{1410} = i \xi e^{i\alpha_e (H+h_w)}, \\
T_{1411} &= i \beta_e e^{-i\beta_e (H+h_w)}, T_{1412} = -i \beta_e e^{i\beta_e (H+h_w)}, T_{1413} = -i \xi e^{-\lambda_1 (H+h_w)}, T_{1414} = -i \xi e^{-\lambda_2 (H+h_w)}, T_{1415} = -i \xi e^{-\lambda_3 (H+h_w)}, \\
T_{1416} &= -r e^{-r(H+h_w)}, T_{1513} = \lambda_1 e^{-\lambda_1 (H+h_w)} (\delta_{p1}^1 - 1), T_{1514} = \lambda_2 e^{-\lambda_2 (H+h_w)} (\delta_{p2}^1 - 1), T_{1515} = \lambda_3 e^{-\lambda_3 (H+h_w)} (\delta_{p3}^1 - 1), \\
T_{1516} &= i \xi e^{-r(H+h_w)} (1 - \delta_s^1), T_{1613} = \lambda_1 e^{-\lambda_1 (H+h_w)} (\delta_{p1}^g - 1), T_{1614} = \lambda_2 e^{-\lambda_2 (H+h_w)} (\delta_{p2}^g - 1), \\
T_{1615} &= \lambda_3 e^{-\lambda_3 (H+h_w)} (\delta_{p3}^g - 1), T_{1616} = i \xi e^{-r(H+h_w)} (1 - \delta_s^g).
\end{aligned}$$